Comments on "Simulation analysis of 3D stability of a landslide with a locking segment: A case study of Tizicao landslide in Maoxian County, Southwest China"

RC1: 'Comment on egusphere-2023-28', Hendy Setiawan, 15 Apr 2023

Your manuscript presents stability analysis of a landslide with a locking segment using three rock bridge models i.e., intact rock mass model, Jenning's model, and contact surface model with high strength parameters in the FLAC3D program. Presenting results discussing the effects of locking ratios, strength parameters of sliding surface and locking mass, as well as a comparison of three rock bridge models in addressing the 3D stability of this landslide. No significant objections came to this manuscript. However, some necessary amendments are needed:

1. In conclusion, the simulation results indicate that the landslide is stable overall in current conditions, due to the existence of the locking segment, and is consistent with field deformation and monitoring data. But here we did not find any descriptions of what monitoring data and instruments were installed in the field. Please described.

Response 1: Thank you for your so careful reading. In fact, we monitored the Tizicao landslide for several years. In the landslide body, twenty-four fixed non-prism monitoring points (T1−T24) were deployed to primarily monitor the surface displacement from June 1, 2017, to October 2, 2017, as shown in Fig. 8 in reference Zhou et al., 2022. They covered almost the entire landslide body. These raw data on the surface displacement were processed using the measurement adjustment software DDM to obtain their deformation amplitude and rates. The detailed descriptions of the monitoring data and instruments were presented in reference Zhou et al., 2022, as shown in the following figure:

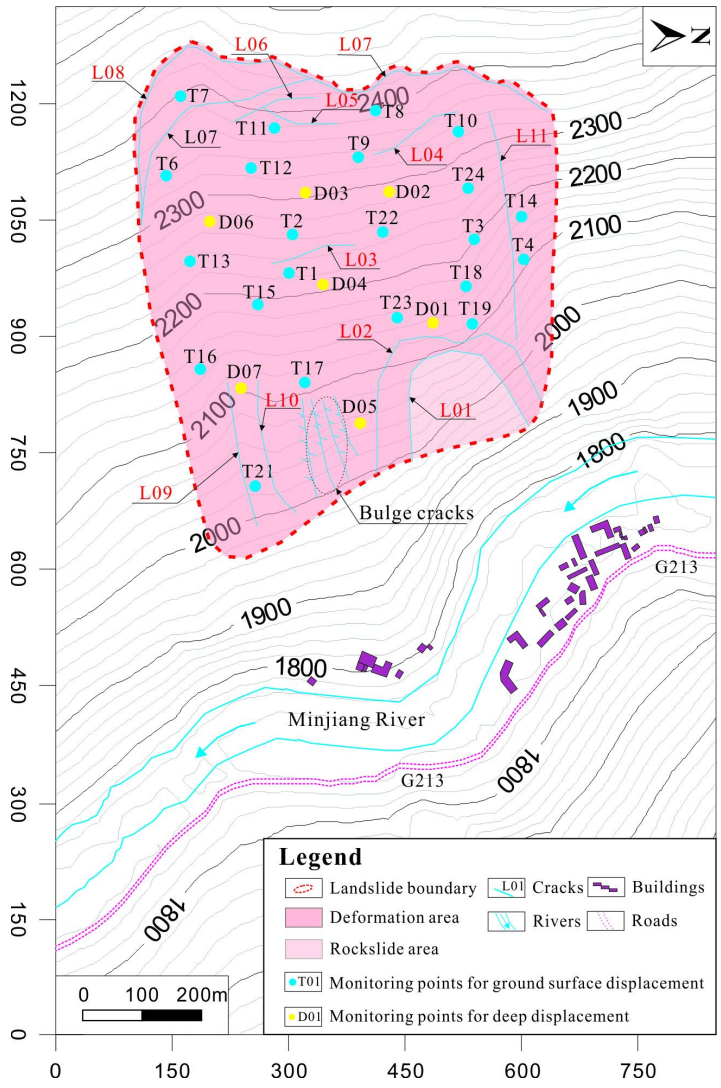

Fig. 1 Plan showing crack development and monitoring point layout in the Tizicao landslide. L01−L11 refer to the numbers of 11 cracks developing in the landslide; besides, there are great numbers of bulging-induced fissures in the middle part of the landslide front; T1−T24 represent 24 fixed non-prism monitoring points; D01−D07 represent seven boreholes used to monitor the deep displacement of the landslide (from Zhou et al. 2022)

The reference is listed as follows:

Zhou, Y. T., Zhao, X. Y., Zhang, J. J., Meng, M. H.: Identification of a locking segment in a high-locality landslide in Shidaguan, Southwest China, Nat. Hazards, 111, 2909–2931, https://doi.org/10.1007/s11069-021-05162-1, 2022.

2. According to Figure 3, there are T1, T2, and T3 for the surface displacement monitoring points, but only T1 have been installed nearby the crack. Then why the contour or isoline map of surface displacement is concentrated on the northeast part of

the landslide where there are no monitoring points (Figure 3b)? Please clarify and give further detailed and concise descriptions of these matters.

Response 2: Thank you for your so careful reading. In the manuscript, we did not describe all the monitoring points in Fig. 3a or the detailed monitoring data in Fig. 3c. As described in "Response 1", twenty-four fixed non-prism monitoring points (T1−T24) were deployed to monitor the surface displacement of the landslide, which was shown in Fig. 8 in reference Zhou et al., 2022. Then, the 24 monitoring curves were obtained to plot the isoline map of surface displacement (Fig. 3b). Figure 3b was also cited from reference Zhou et al., 2022. In Figures 3a and 3c, three monitoring points (T1, T2, and T3) were just used to show the deformation tendency of the landslide, also they are plotted in the isoline map of surface displacement.

3. Methods section only presents numerical 2D and 3D simulations but not yet describing monitoring instruments and laboratory tests (if you use parameters from the tests for the numerical simulation). Please confirm.

Response 3: Thanks for your suggestion. The monitoring instruments are not described in the manuscript because the monitoring instruments and the monitoring data are described in reference Zhou et al., 2022, which was cited in this study. We took the rock samples from the sliding body, sliding bed, and sliding surface of the landslide to conduct the geotechnical tests. The obtained rock parameters (Table 1) were used for the numerical simulation. Among them, the rock density was obtained using the wax-sealing method; the Young's modulus, Poisson's ratio, internal friction angle, and cohesion of rocks were collected from the triaxial test; and the tensile strength was obtained from the Brazilian test. We have added the descriptions of the laboratory tests in section "3.2 3D stability simulations" in the revised manuscript. Please see the text marked in red for details. Thanks.

4. Page 5 Lines 34-35, "The simulation parameters of the sliding body, sliding bed, and sliding surface in the model were obtained through indoor geotechnical tests, shown in Table 1". What kind of geotechnical tests? Please describe.

Response 4: Thanks for your suggestion. The obtained rock parameters (Table 1) were used for the numerical simulation. Among them, the rock density was obtained using the

wax-sealing method; the Young's modulus, Poisson's ratio, internal friction angle, and cohesion of rocks were collected from the triaxial test; and the tensile strength was obtained from the Brazilian test. We have added the descriptions of the laboratory tests in section "3.2 3D stability simulations" in the revised manuscript. Thank you.

5. Page 6 Lines 4-5, the parameters of tensile strength, shear stiffness, and normal stiffness of the sliding surface for the JM model are assumed or based on the laboratory experiment. Please describe what kind of experiment.

Response 5: For the JM model, the landslide was simulated by assigning equivalent shear strength parameters to the contact surface model (S3), as shown in Fig. 9b. Then, the rock bridge and sliding surface were assumed as homogeneous contact surfaces, so the parameters of the assumed contact surfaces were not set as the same parameters of the rock bridge or sliding surface. Then, we took the average values of the tensile strength of the rock bridge and the sliding surface, and the real tensile strength of the rock bridge and sliding surface were obtained from the Brazilian test. For the shear stiffness and normal stiffness of the sliding surface in the JM model, there was no direct reference yet, so we referenced the "FLAC3D6.0 Theory and Background". A good rule-of-thumb is that and be set to ten times the equivalent stiffness of the stiffest neighboring zone. The apparent stiffness of a zone in the normal direction is:

$$\max\left[\frac{K+\frac{4}{3}G}{\Delta z_{\min}}\right]$$

where K & G are the bulk and shear moduli, respectively.

The [ ] notation indicates that the maximum value over all zones adjacent to the interface is to be used.

6. Page 6 Lines 8-10, the strength parameters and stiffness coefficients of the sliding surface in the CSM-HSP and the IRMM were set the same. Could you please explain why?

Response 6: For the IRMM, the sliding surface (S2) was replaced with the contact surface (Fig. 9a); for the CSM-HSP, the sliding surface (S5) was simulated using the contact surface

(Fig. 9c), too. Then, the sliding surface model and its simulation parameters were the same in the FLAC3D program. For the CSM-HSP and the IRMM, only the rock bridge model was different.

7. Please consider the bar scale in the map of Sichuan Province in Figure 1.

Response 7: Thank you for your suggestion. We have added the bar scale in Figure 1.

8. Correct me if Figure 2b is an aerial/oblique view of the landslide? is it necessary to put a bar scale? I prefer to provide a bar scale for Figure 2a as it is an orthogonal image. Please confirm.

Response 8: Figure 2b is an oblique view of the landslide. It is necessary to put a bar scale and we added it in Figure 2b. We also added a bar scale in Figure 2a.

9. In Figure 4a, section A-A' the L07 should be L04, while in Figure 4b L11 not indicated in section B-B'. Then Figure 4c the monitoring points of T1 and T2 nearby L03 are not present. Please revised.

Response 9: Thank you for your so careful reading. In fact, the L07 is not the L04 in section A-A' in Figure 4a, and we carelessly forgot to mark the L04, which has been added in Figure 4a. The L11 was not indicated in section B-B', and we have revised Figure 4b. In Figure 4c, we added the monitoring points of T1 and T2 nearby L03. Please see the revised Figure 4 for detail. Thanks.

10. Location of borehole zk20 provided in Figure 5 is not shown on the map in Figure 3. Please add and clarify.

Response 10: Thank you for your so careful reading. We have added the location of borehole zk20 in Figure 3 in the revised manuscript.

11. Locations of zk08 in Figure 7a and exposed phyllites in Figures 7b and 7c are also not pointed on the map. Please add and clarify.

Response 11: Thank you for your so careful reading. We added the location of borehole zk08 in Figure 3a. The exposed phyllites in Figures 7b and 7c have also been pointed in Figure 3a.

12. Please provide a full description of each abbreviation in the caption of Figure 9.

Response 12: Thank you for your suggestion. The full descriptions of abbreviations IRMM, JM, and CSM-HSP are the intact rock mass model, the Jennings model, and the contact surface model with high strength parameters, respectively. We have added the full description of each abbreviation in the caption of Figure 9.

13. It is not clear whether the red zone of the sliding surface in Figure 10 is shown in the mesh model. Please clarify.

Response 13: The red zone represents the sliding surface in the mesh mode in Figure 10. Because of the opacity of the sliding body mesh, the full view of the red zone of the sliding surface can't be observed. But we can see the full view in Figures 12b-d. Thanks.

14. Cohesion between A-A', B-B' and C-C', D-D' in Figure 11 for 2D simulation are very different significantly, why? Check also its relation with simulation parameters in Table 1. Please discuss.

Response 14: The differences in cohesion between A-A', B-B' and C-C', D-D' in Figure 11 for 2D simulation are caused by the locking ratio k_L (the ratio of the surface area of the rock bridge to the total sliding surface area). For sections A-A' and B-B', the locking ratio $k_L = 0$, i.e., there was no rock bridge in these sections. Then, the shear strength parameters of the sliding surface can be set at the same values as those in Table 1. However, for sections C-C' and D-D', the locking ratios $k_L = 0.23$ and 0.26, respectively. According to the JM model, the slope stability wass calculated by assigning the equivalent shear strength corresponding to different penetration rates to the potential sliding surface. The equivalent shear strength parameters can be calculated as follows:

$$c_{eq} = (1-k)c_r + kc_j \tag{1}$$

$$\tan\varphi_{eq} = (1-k)\tan\varphi_r + k\tan\varphi_j \tag{2}$$

where c_{eq} and φ_{eq} are the equivalent cohesion and the equivalent friction angle, respectively; φ_r and φ_j represent the friction angles of an intact rock and joints, respectively, and c_r and c_j are the cohesion of an intact rock and joints, respectively.

Considering that co-planar joints are separated by the intact rock bridge, the relative quantity of intact rocks along the sliding surface can be expressed as the ratio k, which is defined as follows (Jennings, 1970):

$$k = \frac{\sum A_j}{\sum A_j + \sum A_r} = 1 - k_L \quad (3)$$

where $\sum A_j$ denotes the surface area of joints, $\sum A_r$ is the surface area of the rock bridge, and k_L is the locking ratio (the ratio of the surface area of the rock bridge to the total sliding surface area).

So, we used equivalent cohesion c_{eq} and equivalent friction angle φ_{eq} when calculating the 2D Fos. The equivalent shear strength parameters were obtained from equations (1) and (2) based on the shear strength parameters of the rock bridge and the sliding surface in Table 1, as well as the different locking ratios in Figures 11c-d. The equivalent shear strength parameters are shown in Figures 11c-d.

15. Contours of shear displacement and intense deformation zone in Figure 12 seems not in line with the isoline map of surface displacement in Figure 3b. Perhaps unclear explanation in the text that I could not catch. Could you emphasize the above results?

Response 15: Sorry for the unclear explanation of the deformation characteristics between the simulation results in Fig. 12 and the isoline map of surface displacement in Fig. 3b. We added the characteristics of the surface displacement in Fig. 3b, which are described as follows:

As shown in the isoline map of surface displacement (Fig. 3b), a sliding event occurred in a general northeast direction (closer to the north) from August 13, 2017 to January 25, 2018. In this event, the maximum surface displacement (1210 mm) occurred at the northern toe, which coincided with the location where the front collapsed (Fig. 2d). The landslide's rear and middle parts showed similar surface displacement of 150–300 mm in the sliding event, indicating that they slid as a whole. The minimum surface displacement of 30–150 mm occurred in the southern area of the slope toe throughout the whole sliding event. Therefore, the southern area serves as the anti-sliding area of the whole landslide.

Figs. 12a and 3a show different displacement values because the monitoring data obtained from August 13, 2017 to January 25, 2018 (after the large deformation in July 2017) do not include the complete deformation data of the landslide. However, Figs. 12a and 3a reflect the same deformation tendency.

16. Font remark in Figure 13 is not visible, please change its color.

Response 16: Thanks for your suggestion. We have changed the yellow color into black in Figure 13.

17. The locking segment needs to be described further, is it generated due to the movement characteristic of a landslide? Or originally due to the lithological or geological conditions? Or are there any factors or settings that cause this feature? Please discuss.

Response 17: Thanks for your suggestion. In section "2. Study site", we described the location, area, lithology, RQD values at different depths, and surface deformation characteristics of the locking segment. However, we did not describe the origin cause of the locking segment.

In fact, Zhou et al. (2022) preliminarily discussed the cause. The locking masses of the Tizicao landslide occur on the convex bank, while the non-locking masses have developed on the concave bank, indicating that the locking masses are directly related to the S-shaped river valley under the landslide. From a geomorphological point of view, landslides rarely occur on convex banks but occur more frequently on concave banks. From a topographical perspective, a convex slope is more stable than a concave slope under the same conditions. Noticeably, the concave and convex banks of the S-shaped valley under the Tizicao landslide differ greatly in slope and lithology. Therefore, the rock masses on the south side of the landslide above the convex bank are intact and constitute the potential locking segment of the landslide.

We added the above descriptions in section "2. Study site" to explain the cause of the locking segment.